

# Magnetic structure refinement with neutron powder diffraction data using GSAS: A tutorial

J. Cui

*Materials Analysis and Chemical Sciences, GE Global Research Center, Niskayuna, New York*

Q. Huang

*NIST Center for Neutron Research, National Institute of Standards and Technology, Gaithersburg, Maryland*

B. H. Toby

*Advanced Photon Source, Argonne National Laboratory, Argonne, Illinois*

(Received 20 December 2005; accepted 27 January 2006)

Neutron diffraction provides a direct probe for the ordering of spins from unpaired electrons in materials with magnetic properties. The ordering of the spins can be modeled in many cases by adding spin directions to standard crystallographic models. This requires, however, that crystallographic space groups be extended by addition of a “color” attribute to symmetry operations, which determines if the operation maintains or flips the direction of a magnetic spin. Rietveld analysis provides a mechanism for fitting magnetic structure models to powder diffraction data. The general structure and analysis system (GSAS) software suite is commonly used for Rietveld analysis and includes the ability to compute magnetic scattering. Different approaches are commonly used within GSAS to create models that include magnetism. Three equivalent but different approaches are presented to provide a tutorial on how magnetic scattering data may be modeled using differing treatment of symmetry. Also discussed is how magnetic models may be visualized. The commands used to run the GSAS programs are summarized within, but are shown in great detail in supplementary web pages. © 2006 International Centre for Diffraction Data. [DOI: 10.1154/1.2179805]

Key words: magnetic structure, Rietveld analysis, powder diffraction, crystallographic education, neutron scattering

## I. INTRODUCTION

Neutrons are extremely valuable as a probe of materials structure. Neutrons are scattered by atomic nuclei and typically have better sensitivity to light atoms than X rays, which are scattered by electrons. Further, nuclear scattering cross sections for neutron scattering do not vary with  $\sin \theta/\lambda$ , so neutrons provide scattering information over a wider diffraction range than X rays. However, neutrons also have a non-zero spin and this causes them to be scattered by the spin of unpaired electrons, when such electrons are present. When materials exhibit magnetic properties, this is typically due to long-range ordering of these unpaired electrons; in these cases, neutrons will be scattered coherently from the electrons in the ordered domains, just as neutrons are scattered by the nuclei of atoms. The terms nuclear scattering and magnetic scattering (better labels would be nuclear diffraction and magnetic diffraction) are used to separate diffraction from atoms versus unpaired electrons. The contributions are assigned as arising from the “nuclear structure” and “magnetic structure,” respectively. While, as noted before, nuclear-scattering cross sections are constant, magnetic-scattering cross sections decrease with  $\sin \theta/\lambda$ , similar to X-ray scattering, though form factors differ since X rays scatter from all electrons, while magnetic scattering of neutrons occurs from valence electrons. The fact that neutrons have a relatively strong interaction with unpaired electrons increases their value considerably as a probe of magnetic materials.

The ability to model both nuclear and magnetic structures in powder diffraction data was central to the develop-

ment of the Rietveld technique. Hugo Rietveld’s initial Algor program for full profile fitting was able to model both nuclear and magnetic structures (Rietveld, 1969). However, a description of magnetic ordering requires more sophistication than what is needed for structural descriptions. It should be mentioned, however, that powder diffraction can be of limited power in determining the details of magnetic ordering, due to overlap of symmetry-related reflections. For example, in a tetragonal system, the powder diffraction pattern arising from a set of atoms with moments in the  $a$  [or (100)] direction will be identical to that where the moments are in the  $a+b$  [or (110)] direction. In fact, rotating the spin arrangement to any angle in the  $ab$  plane will leave the powder diffraction intensities unchanged (Shirane, 1959). Only single crystal measurements will demonstrate a difference between the two models.

To describe the spin direction associated with an atom, two different conventions are used. Frequently, the spin is considered as an ordinary (polar) vector, where the vector magnitude is equal to the spin moment. For magnetic symmetry, an alternate approach is used, where the spin is described as an axial vector associated with a current loop. In this case, the axial vector direction is normal to the plane of the loop and by convention points toward a viewer who sees the loop rotation in the clockwise direction. These two ways of describing a vector differ when the application of symmetry is considered. As an example, a center of symmetry will invert the direction of a polar vector, but not the direction of rotation of a current loop; however, while the position of an axial vector will be changed by a center of symmetry, the

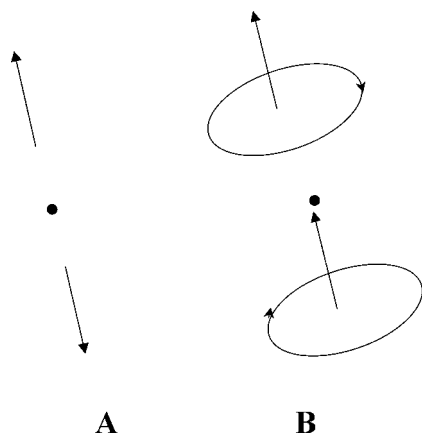


Figure 1. The effect of a center of symmetry (indicated by the filled circle) on (A) a polar vector and (B) an axial vector. Note that the loop direction associated with the axial vector remains clockwise after inversion, so the vector direction is unchanged. By contrast, the center inverts the direction of the polar vector.

direction of an axial vector will not be changed. This is illustrated in Figure 1. By contrast, a rotation axis will invert the direction of an axial vector, but not a polar vector. Good illustrations showing the effect of other classes of symmetry operations on axial vectors can be found in literature (Donnay *et al.*, 1958; Cox, 1972).

For treatment of the symmetry of magnetic systems, traditional crystallographic space group theory is extended using color or Shubnikov (also called Heesch) space-group theory (Heesch, 1930; Shubnikov and Belov, 1964; Vainshstein, 1996). Traditional crystallographic symmetry operations treat objects as collections of points, and the only effect of a symmetry operation on a point can be to displace it, since a point has no directionality. Complex objects can be considered as a collection of points; the effect of crystallographic symmetry on the object is the same as would be obtained by transforming each constituent point individually. Color space group theory adds extra rules for treating the direction associated with magnetic vectors. The effect of a color symmetry operation on a magnetic vector may thus be different from the effect of that operator on an object. Magnetic symmetry operations are given an additional attribute, a “color”—either red or black—where a “black” operation applies symmetry directly to the vector; while a “red” operation applies the same symmetry, but also adds a spin inversion and thus gives the opposite spin direction of the black. The spin flip performed by a red operation is sometimes referred to as “time reversal.” The prefix “anti-” is commonly applied to differentiate red operators from black ones, so that a red mirror plane would be labeled as an antimirror, etc.

By convention, the effect of color symmetry is defined by action on axial vectors, *not polar vectors*. As noted before, a black center of symmetry does not change the direction of an axial vector, so a red center of symmetry will reverse this direction. Color space group theory also allows lattice-centering operations to be red or black. While traditional Bravais lattices only allow for body and face centering, color space groups also allow antientering on cell edges, as this simplifies treatment of lattice doubling, as occurs in simple antiferromagnetic systems.

Not all combinations of color symmetry operations are internally consistent; but for most of the 230 standard crystallographic space groups, there will be more than one choice for how to apply color. This, plus the additional centering, results in 1651 color space groups. Color space groups are named using the standard Hermann–Mauguin name for the base space group, except that red operations that appear in the space group name are marked with an apostrophe ('). For example, the color space-group  $Pm'mm$  has the same symmetry operations as the standard  $Pmmm$  space group except that the  $m'mm$  indicates that the mirror plane perpendicular to  $a$  is red while the mirror planes perpendicular to  $b$  and  $c$  are black.

It is worth noting that magnetic ordering frequently breaks the symmetry of the nuclear structure, but in many cases, the lattice and nuclear structure parameters for such systems often remain unchanged from the higher symmetry, within the precision of all experimental technique measurements. For example, consider a tetragonal material where all magnetic moments are aligned in any one direction in the  $a$ - $b$  plane. This magnetic ordering breaks tetragonal symmetry since this ordering is inconsistent with a four-fold axis; the resulting magnetic structure will thus be orthorhombic. Nonetheless, the nuclear structure may retain four-fold symmetry. For this reason, it is often necessary to constrain the nuclear structure to higher symmetry than the magnetic structure, leading to potential complexity in performing magnetic refinements.

It should be noted that in real life, far more complex things may happen than mere lattice doubling: The spin ordering may repeat over longer length scales, or the nuclear and magnetic lattices may be incommensurate. An alternate description of magnetic ordering that derives from a treatment of symmetry, known as representational analysis provides a more comprehensive mechanism for modeling magnetic structures (Kovalev, 1993; Iziumov and Syromiatnikov, 1990). In this method, magnetism is described in terms of a magnetic propagation vector and the irreducible representations (irreps) that comprise the space group. A number of software tools, notably MODY (Sikora *et al.*, 2004), SARAH (Wills, 2000), ISOTROPY (Stokes and Hatch, 2002), and BasiReps (Rodríguez-Carvajal, 2004) are available for exploring magnetic symmetry. Indeed, representational analysis combined with Landau theory can be used to tabulate all possible magnetic structures for a system (Wills, 2002). The FullProf package implements irreps for modeling magnetic systems and thus is probably the tool of first choice for use by experts (Rodríguez-Carvajal, 1993). The level of group theory needed for this approach is well beyond the scope of this article, alas.

This article is intended as a practical guide on how magnetic Rietveld refinements are performed with neutron powder diffraction data using the Generalized Structure and Analysis System (GSAS) suite of Rietveld software (Larson and Von Dreele, 2000) and where possible using the EXPGUI graphical user interface (Toby, 2001). Together, GSAS and EXPGUI are widely used for Rietveld refinement (Fultz and Billinge, 2004). When a magnetic structure is modeled in GSAS, all standard crystallographic symmetry operations can be flagged as either red or black. However, GSAS does not implement edge centering at present.

(Experienced GSAS users may remember an option for lattice doubling operations that effectively allowed direct representation of color space groups. Due to problems with the implementation of lattice doubling, the feature has been disabled). Different approaches are used within GSAS to model nuclear and magnetic structures. This paper will present three different approaches for a single system. In one example, a single model will be used to describe both the magnetic and crystallographic scattering, adapting the nuclear model to fit the symmetry to that of the magnetic model. In a second example, the nuclear and magnetic models will be treated separately, each using the symmetry appropriate to that model. In a third example, only lattice symmetry operations are used to describe the magnetic model. This latter approach may be abhorrent to the crystallographer, but is often convenient to the physicist who wishes to explore possible magnetic models without deriving the corresponding symmetry. The specific details for performing each step is shown in an accompanying set of web pages.

As is the case with determining starting models for Rietveld refinements of crystal structures, determining trial models for magnetic structures is a complex problem, sometimes solved through analogy to related systems, intuition, modeling, analysis software, or trial and error approaches. The goal of this paper is to show how models may be tested and refined, but does not explore how they are derived.

## II. EXPERIMENTAL DATA AND STARTING MODELS

### A. Neutron diffraction data

The example data used in this document were collected on a sample of  $\text{YBa}_2\text{Fe}_3\text{O}_8$  at room temperature using the high-resolution neutron powder diffractometer, BT-1, at NIST. Details of sample preparation and neutron diffraction measurements, including a more complete discussion of the original crystallographic analysis, can be found elsewhere (Huang *et al.*, 1992; Karen *et al.*, 2003).

### B. Approximate nuclear structure of $\text{YBa}_2\text{Fe}_3\text{O}_8$

The nuclear structure of  $\text{YBa}_2\text{Fe}_3\text{O}_8$  is depicted in Figure 2. The crystallographic data and fractional coordinates of the atoms are listed in Table I.

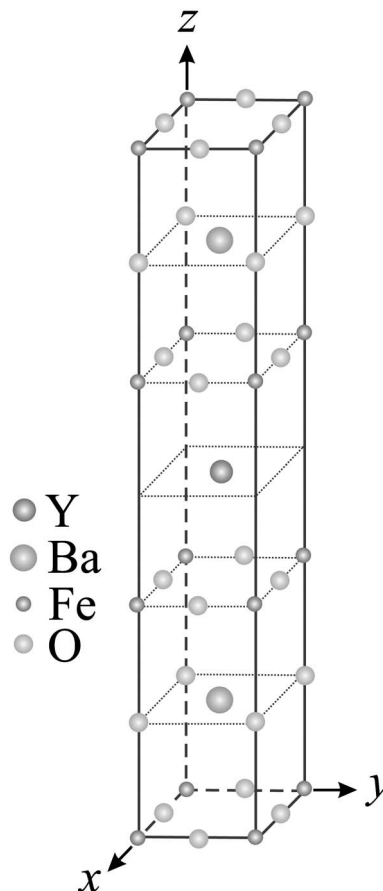


Figure 2. Nuclear structure of  $\text{YBa}_2\text{Fe}_3\text{O}_8$ .

### C. Trial magnetic structure of $\text{YBa}_2\text{Fe}_3\text{O}_8$

$\text{YBa}_2\text{Fe}_3\text{O}_8$  is antiferromagnetic at room temperature. A proposed model has the magnetic moments on the iron atoms with alternating spins of equal magnitude, either parallel or antiparallel to the  $a$  axis of the nuclear cell, with spin directions as illustrated in Figure 3. While this model appears to have a fairly simple and small unit cell, this is misleading because there are two inequivalent planes of iron atoms (Fe1 versus Fe2). Figure 4 shows a section of the neutron powder diffraction data collected for  $\text{YBa}_2\text{Fe}_3\text{O}_8$ , along with intensities computed from the nuclear model in Table I and from the magnetic model in Figure 3.

TABLE I. Atom positions as fractional coordinates for  $\text{YBa}_2\text{Fe}_3\text{O}_8$ . The space group is  $Pm\bar{m}m$  and approximate lattice constants are  $a=3.925 \text{ \AA}$ ,  $b=3.907 \text{ \AA}$ ,  $c=11.786 \text{ \AA}$ .

Element	Label	$x$	$y$	$Z$	Multiplicity	Occupancy
Y	Y1	1/2	1/2	1/2	1	1
Ba	Ba1	1/2	1/2	0.167	2	1
Fe	Fe1	0	0	0	1	1
Fe	Fe2	0	0	0.34	2	1
O	O1	0	0	0.181	2	1
O	O2	1/2	0	0.383	2	1
O	O3	0	1/2	0.380	2	1
O	O4	0	1/2	0	1	0.853
O	O5	1/2	0	0	1	0.978

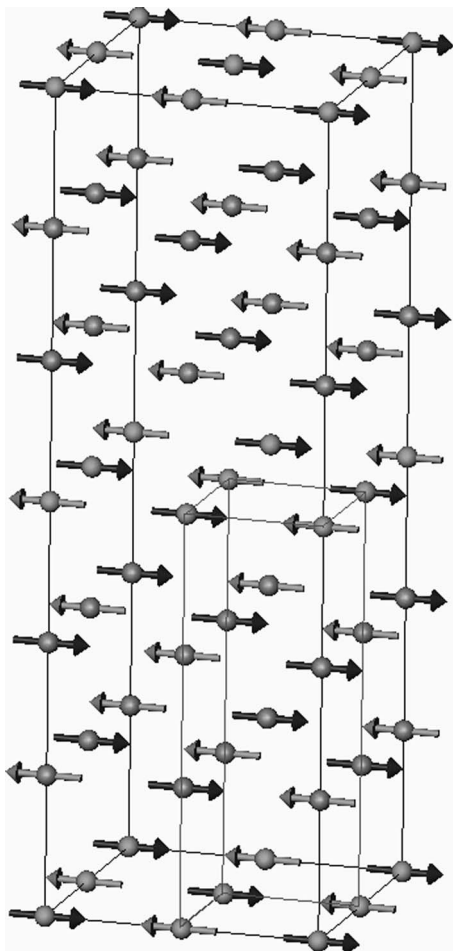


Figure 3. Spin orientations for  $\text{YBa}_2\text{Fe}_3\text{O}_8$ . Spin directions are shown as arrows, with spins parallel to  $a$  in black and antiparallel spins in gray. The Fe1 atoms are in the top, bottom, and central planes. The unit cell for this structure represents a doubling of each lattice constant of the nuclear cell, which is shown in Fig. 2. The magnetic cell and nuclear cell are the outer and inner outlined boxes, respectively.

### III. ASSIGNMENT OF MAGNETIC SYMMETRY

The magnetic structure can be described as a  $2 \times 2 \times 2$  expansion of the  $Pmmm$  cell, where the lattice points in the original cell populate either lattice points, edge centers, face centers, or body centers in the new lattice (edge and face centers occur on all axes). The edge centers and body center would have red (inverting symmetry), while the face centers are black. The addition of seven centering operations to the identity operator increases all site multiplicities eightfold, which offsets the eight-fold ( $2 \times 2 \times 2$ ) increase in cell volume relative to the nuclear cell description. Thus, in this description, with edge, face, and body centers, the asymmetric unit volume in the nuclear and magnetic cell can be the same.

Since GSAS does not at present support edge centers, we must find a description without them. We can do this with only the black face centers. Since we have lost one-half of the centering operations, the magnetic asymmetric unit will be at least double that of the nuclear asymmetric unit. Since  $Fmmm$  is a maximal isomorphic subgroup of  $Pmmm$  with all axes doubled, choosing this space group will lead to the least reduction in symmetry (Billiet *et al.*, 2004). So, we are pre-

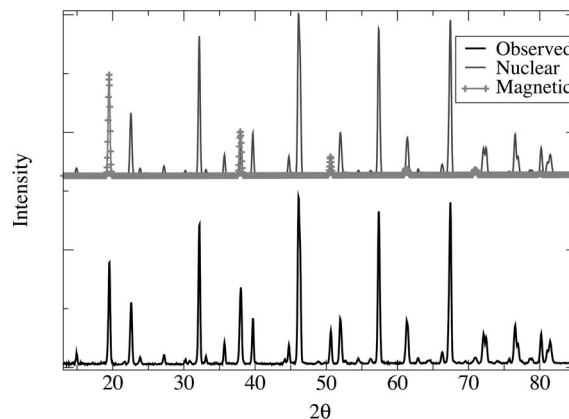


Figure 4. Observed and simulated neutron powder diffraction data for  $\text{YBa}_2\text{Fe}_3\text{O}_8$ . A section of observations is shown in the lower plot, while intensities simulated considering magnetic diffraction and nuclear scattering separately are shown above. The magnetic intensities are marked with crosses; note their much faster decrease in strength.

sented with the task of finding the color space group description of the spin arrangement in  $Fmmm$ . The primary symmetry operators in this space group are the three mirror planes that are perpendicular to the  $a$ ,  $b$ , and  $c$  axes, so the colors of these operators must be determined. It should be noted that the Fe1 atoms lie on all three of these mirror planes and the Fe2 atoms lie on the mirror planes perpendicular to both  $a$  and  $b$  ( $m_x$  and  $m_y$ , respectively).

The reader is directed to papers by either Donnay *et al.* (1958) or Cox (1972) for a valuable general presentation on how colored symmetry operations affect spin directions. However, the case of mirror planes is fairly straightforward. A black mirror plane will preserve the component of spin that is perpendicular to the mirror plane, while inverting the components parallel to the plane. A red antimirror plane will invert any component of spin that is perpendicular to the mirror plane, while preserving the components parallel to the plane. This means that an atom lying on a black mirror plane can only have a magnetic moment perpendicular to the plane, as illustrated in Figure 5. Likewise, an atom lying on a red antimirror plane may not have a moment component outside the plane. Since the Fe1 atoms have moments in the  $\pm a$  direction and lie on the  $m_y$  and  $m_z$  mirror planes, where the magnetic spin is contained in each plane, the color for both operators must be red. Similarly, for both Fe1 and Fe2, the spin is perpendicular to the  $m_x$  plane, so the  $m_x$  operator

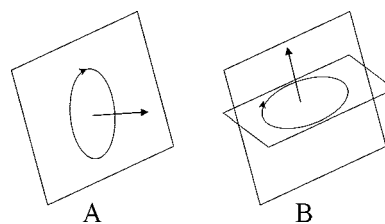


Figure 5. Restrictions on operator color when spins are located on a mirror plane. In case A, the spin is perpendicular to the mirror plane, so the current loop is contained in the plane; the mirror must have black (noninverting) symmetry. In case B, the spin is contained in the plane and the loop is perpendicular to the mirror plane; the mirror must have red (inverting) symmetry.

TABLE II. Fractional coordinates for  $\text{YBa}_2\text{Fe}_3\text{O}_8$  in supergroup  $Fmmm$ .

Element	Label	$x$	$Y$	$z$	Multiplicity	Occupancy
Y	Y1	1/4	1/4	1/4	8	1
Ba	Ba1	1/4	1/4	0.167/2	16	1
Fe	Fe1a	0	0	0	4	1
Fe	Fe1b	0	0	1/2	4	1
Fe	Fe2a	0	0	0.34/2	8	1
Fe	Fe2b	0	0	1/2-(0.34/2)	8	1
O	O1a	0	0	0.181/2	8	1
O	O1b	0	0	(0.181/2)-1/2	8	1
O	O2	1/4	0	0.383/2	16	1
O	O3	0	1/4	0.380/2	16	1
O	O4	0	1/4	0	8	0.853
O	O5	1/4	0	0	8	0.978

color must be black. Thus, the Shubnikov symmetry must be  $Fmm'm'$ . Note that the black  $m_x$  operator is inconsistent with any magnetic moment in the  $b$  or  $c$  directions for both Fe1 and Fe2, thus these moments are locked along the  $\pm a$  direction.

The remaining task is to determine the locations of the magnetic atoms in this transformed lattice. In the general case, the transformation matrix that is applied to the unit-cell vectors, as well as any offset to the origin, must be determined. The inverse of this matrix is then applied to the fractional coordinates, followed by addition of the origin offset in order to obtain the fractional coordinates in the new setting. In the case where the asymmetric unit increases, it is also necessary to identify the atoms that must be repeated in the new model. This can be done intelligently by determining the identity of the symmetry element(s) that are lost in the transform and then transforming the positions both with and without application of that symmetry, or by brute force by transforming the contents of multiple units cells to the new setting, determining which sets of atoms are related by symmetry, and then retaining only one position from each set.

In this case, where the axes relationships are trivial and there is no origin offset, it is easy to perform the coordinate transformation. Slightly more thought is needed to determine a set of atoms to make up an asymmetric unit in the new setting; the coordinates for one choice are provided in Table II. These were obtained by applying symmetry operations to the asymmetric unit contents in  $Pmmm$ , applying unit cell translations to generate all atoms in the  $Fmmm$  unit cell, transforming the coordinates to the larger cell, and then testing each generated position to determine which positions are symmetry-related in the  $Fmmm$  setting. The spins needed to

TABLE III. Fractional coordinates and moment for the magnetic atoms in space group  $Fmm'm'$ . Moments are in the  $a$  direction. The  $z$  coordinate is expressed in terms of the atom position ( $z_p \approx 0.34$ ) in the  $Pmmm$  nuclear structure.

Label	$x$	$Y$	$z$	Moment
Fe1a	0	0	0	$3.5\mu_B$
Fe1b	0	0	1/2	$-3.5\mu_B$
Fe2a	0	0	$z_p/2$	$-3.5\mu_B$
Fe2b	0	0	$1/2-z_p/2$	$3.5\mu_B$

construct the magnetic scattering are shown in Table III. Likewise, for the GSAS model where no magnetic symmetry will be applied, a list of all magnetic atoms in the unit cell is needed. These can be obtained by applying the  $Fmmm$  symmetry operations to the atom positions in Table II to obtain the coordinates shown in Table IV.

It may occur to the reader that the spins can be described in a primitive unit cell (constructed from vectors from the origin to the three face centers) or a body-centered unit cell (constructed from the face centers in one plane without changing the lattice in the perpendicular direction). It should be noted that these cells have triclinic and monoclinic sym-

TABLE IV. Fractional coordinates and moment for all magnetic atoms in the  $2 \times 2 \times 2$  expanded unit cell (space group  $P1$ ). Magnetic moments are in the  $a$  direction and have units of  $\mu_B$ . The  $z$  coordinates are computed assuming the Fe2 atom position has  $z=0.34$  in the  $Pmmm$  parent structure.

Label	$x$	$y$	$z$	Moment
Fe1a1	0	0	0	3.5
Fe1a2	1/2	1/2	0	3.5
Fe1a3	1/2	0	1/2	3.5
Fe1a4	0	1/2	1/2	3.5
Fe1b1	0	0	1/2	-3.5
Fe1b2	1/2	1/2	1/2	-3.5
Fe1b3	1/2	0	0	-3.5
Fe1b4	0	1/2	0	-3.5
Fe2a1	0	0	0.17	-3.5
Fe2a2	1/2	1/2	0.17	-3.5
Fe2a3	0	0	-0.17	-3.5
Fe2a4	1/2	1/2	-0.17	-3.5
Fe2a5	1/2	0	0.33	-3.5
Fe2a6	0	1/2	0.33	-3.5
Fe2a7	0	1/2	-0.33	-3.5
Fe2a8	1/2	0	-0.33	-3.5
Fe2b1	1/2	0	0.17	3.5
Fe2b2	0	1/2	0.17	3.5
Fe2b3	1/2	0	-0.17	3.5
Fe2b4	0	1/2	-0.17	3.5
Fe2b5	0	0	0.33	3.5
Fe2b6	1/2	1/2	0.33	3.5
Fe2b7	0	0	-0.33	3.5
Fe2b8	1/2	1/2	-0.33	3.5

metry, respectively, and will thus not reflect the higher lattice symmetry of the magnetic and nuclear models.

#### IV. FITTING MAGNETIC STRUCTURES

Since magnetic scattering occurs from a separate mechanism than nuclear scattering, computation of these two parts of the total diffraction can be performed separately. GSAS allows a crystallographic phase to be used for the computation of nuclear scattering, magnetic scattering, or both. This allows a magnetic system to be modeled via a number of approaches. In the following sections, three different approaches to modeling the same system will be used. In the first two examples, a crystallographic phase that provides only nuclear scattering will be modeled with the observed crystallographic symmetry,  $Pmmm$ . The magnetic phase will be modeled in two different ways: In the first example, the full color space group symmetry will be used in a second phase that will be used for magnetic scattering computation only. Only the atoms that scatter magnetically (Fe1 and Fe2) need to be included in this phase. Some constraints will be required in this example to keep atomic positions and lattice constants comparable between these phases. The second example will be much like the first, except that no symmetry will be used to model the magnetic phase. This approach is cumbersome, in that many additional constraints are needed to prevent correlation from redundant parameters when refining models. However, it can be very helpful for exploring magnetic intensities produced by different magnetic models, and refinements can be easy to perform with simpler systems.

The final example will use a single structural phase for both the nuclear and magnetic scattering components. This requires expansion of the nuclear structure to the  $Fmmm$  unit cell and an understanding of how the site symmetry requirements in  $Pmmm$  are relaxed in  $Fmmm$  so that appropriate constraints can be applied to the crystallographic phase. This example is probably the simplest approach for this system.

Ideally, before beginning the fit of a magnetic material, the nuclear structure will have been investigated under conditions where there is no magnetic scattering. Most commonly, this is done using data that are collected at elevated temperature, or by using X-ray diffraction. For the examples presented here, this has already been done, and these results are reported in Table I. This step is not always needed. The first step in all three of the examples presented here is to refine a model that contains only a nuclear scattering phase. These models provide a reasonable fit, which is quite acceptable as a starting model for the magnetic refinement. The second step in each example is then to introduce the magnetic scattering. The third step is to refine the magnetic parameters. The following sections outline the steps used to perform the refinements using each approach. Where a step can be performed with EXPGUI, the step is described simply. For steps that require the EXPEDT program, the actual EXPEDT commands are included in square brackets, where the symbol “ $\_$ ” indicates a blank line. A set of accompanying web pages go through the same steps, but provide considerably more detail (see <http://www.ncnr.nist.gov/xtal/software/magut>).

It is worth noting that in all of these examples, the models used have symmetry-related but nominally independent parameters. For example, all of the Fe2 atoms in Tables II or III are generated from a single atom site. The data do not support independent refinement of the atomic parameters for the positions generated with lower symmetry. If the attempt is made to refine two (or more) parameters that are indistinguishable, then the GSAS refinement software (GENLES) will recognize the redundancy and will select only one of the related parameters to be refined. On occasion, round-off errors can cause symmetry-related parameters to have nearly identical but slightly differing effects on the fit. In this case, the Hessian matrix is nearly singular and the least-squares algorithm computes extremely large shifts to be applied to the parameters, again due to round-off error in the matrix inversion. Usually when this occurs, the fit becomes substantially degraded in each cycle of refinement. In some cases, the parameter changes are large enough to cause GENLES to crash or to generate parameter values that are so large or small that subsequent GSAS programs cannot be run. It is the user's responsibility to devise constraints to group these duplicated parameters or make sure that they are not refined.

##### A. Approach 1: Two-phase fit using magnetic symmetry

The first step in this approach is to establish a model for the nuclear scattering in space group  $Pmmm$  using the coordinates in Table I and the neutron diffraction data. The following steps are used:

1. In EXPGUI, input the  $Pmmm$  nuclear coordinates.
2. Input the neutron diffraction data and instrument parameter files.
3. Fit the background and scale factor.
4. Add lattice parameters to fit.
5. Add the  $2\theta$  zero correction to fit.
6. Use constraints to group  $U_{iso}$  parameters for like atoms.
7. Fit structural parameters (coordinates,  $U_{iso}$  values and, where appropriate, fractional occupancies) as well as the background, scale, lattice, and  $2\theta$  zero.

Then, a second phase in space group  $Fmmm$  is added to treat the magnetic scattering, constraints are added and the model is refined:

8. Input a new phase with the four Fe atom positions in  $Fmmm$  symmetry shown in Table III. As the information is entered, the cell parameters and Fe2 coordinates are updated to be consistent with the refinement from the  $Pmmm$  structure.
9. In EXPEDT, change the flag on the second phase to be magnetic-only [P P M 2 C].
10. Enter the color flags for the two red magnetic symmetry operations [L A P 2 M S C 2 C 3], and set moments for the atoms in phase 2 [L A P 2 M M 1 3.5 M2 -3.5 M 3 -3.5 M 4 3.5].
11. Check/input the magnetic form factor [L F M F E +3 C .3972 13.244 .6295 4.903 -.0313 .35 0 0 .0044 N U]. Note that magnetic form factors depend strongly on the atom valence (Brown, 1995).
12. Constrain the unit-cell parameters between the two

phases [L O L K I 1, RM11, 4 2, RM11, 1 ↵ I 1, RM22, 4 2, RM22, 1 ↵ I 1, RM33, 4 2, RM33, 1 ↵].

Note that these constraints are applied to the reciprocal lattice tensor, where  $RM11 = a^{*2}$ , etc., so these constraints are related to the inverse of the square of the ratio of the lattice constants.

13. In EXPGUI, constrain the magnetic Fe atoms to have the same position (Fe2a is shifted by 0.5 relative to Fe4, and Fe2b is shifted by -0.5 relative to Fe4); constrain  $U_{iso}$  for all Fe atoms in both phases to be the same.
14. Set the magnetic scattering phase fraction to be one-eighth that of the nuclear phase in EXPGUI, since there are eight times as many atoms in each unit cell of the magnetic phase.
15. Add flags for refinement of the second phase (lattice parameters, coordinates, and  $U_{iso}$  parameters) and refine.
16. Constrain the profile terms to be the same between the two phases; refine adding GU, GV, and GW (U, V, and W) to the model.
17. In EXPEDT, constrain the four Fe magnetic moments to be the same (allowing for the differences in direction) and then set the refinement flag for the magnetic Fe atoms [L A P 2 V 1:4 M]; refine with these additional parameters.

## B. Approach 2: Two-phase fit without magnetic symmetry

The initial steps in this approach are identical to Steps 1–7 in Approach 1. However, all the magnetic atoms in the expanded unit cell are entered to avoid use of color symmetry. The subsequent treatment differs from Approach 1, as significantly more constraints are needed to perform fitting:

8. In EXPGUI, input a new phase with the 24 Fe atoms positions as supplied in Table IV. The cell parameters for this phase are updated to be consistent with the *Pmmm* structure. The position of atom Fe2 in the *Pmmm* phase is reset to be consistent with the corresponding atoms in the magnetic phase.
9. In EXPEDT, change the flag on the second phase to be magnetic only [P P M 2 C].
10. Enter the color editing menu [L A M S X] (no changes are directly made by this action, but magnetic intensities will not be computed for the phase if this step is omitted). Then, set moments for the atoms in phase 2 [L A P 2 M M 1 3.5 M 2 3.5 M 3 3.5... M 24 3.5].
11. Check/input the magnetic form factor [L F M FE +3 C .3972 13.244 .6295 4.903 -.0313 .35 0 0 .0044 N U].
12. Constrain the unit-cell parameters between the two phases and “hold” the unit-cell angles for the magnetic cell (since they are not constrained by symmetry) [L O L K I 1, RM11, 4 2, RM11, 1 ↵ I 1, RM22, 4 2, RM22, 1 ↵ I 1, RM33, 4 2, RM33, 1 ↵ X I F RM12 I RM13 I RM23].
13. In EXPGUI, constrain the magnetic Fe atoms to have the same position (atoms at  $z=0.17$  and  $z=-0.33$  shift at 50% of Fe4, while atoms at  $z=-0.17$  or  $z=0.33$  shift at -50% of Fe4). Constrain all Fe atoms in both phases to have the same  $U_{iso}$  value.
14. In EXPEDT, fix the  $x$  and  $y$  parameters of the Fe atoms,

since they are not fixed by symmetry [L A P 2 F I 9 X I 9 Y I 10 X I 10 Y... I 24 Y].

15. Set the magnetic scattering phase fraction to be one-eighth that of the nuclear phase in EXPGUI, since there are eight times as many atoms in each unit cell of the magnetic phase.
16. Add flags for refinement of the second phase (lattice parameters, coordinates, and  $U_{iso}$  parameters) and fit.
17. Constrain the profile terms to be the same between the two phases; refine adding GU, GV, and GW (U, V, and W) to the model.
18. In EXPEDT, constrain the 24 Fe magnetic moments to be the same (allowing for the differences in direction). Set the refinement flag for the magnetic Fe atoms. Delete the holds on the magnetic Fe atom  $x$  and  $y$  coordinates (because GSAS only allows 72 atom parameters to be fixed; use of more causes EXPEDT to crash with no error message). Then, input holds on the moment components in the  $y$  and  $z$  directions [L A P 2 V 1:24 M F D 1:32 I 1 MY I 1 MZ I 2 MY ... I 24 MZ]. In EXPGUI, turn off the coordinate refinement flag for the Fe atoms in both phases. Refine with these additional parameters.

## C. Approach 3: Single-phase fit with magnetic symmetry

In this example, the nuclear scattering is modeled using a supergroup. This requires some extra work in setting up constraints and in fixing parameters for the initial fit, but simplifies the effort of modeling the magnetic scattering. The first step in this approach is to determine the asymmetric unit for the supergroup structure, which is given in Table IV, and to determine the parameters that are linked in the model, as well as the parameters that must be fixed because symmetry in the parent group does not allow them to be varied. The following steps are then used to perform the refinement:

1. In EXPGUI, input the *Fmmm* nuclear coordinates.
2. Input the neutron diffraction data and instrument parameter files.
3. Fit the background and scale factor.
4. Add lattice parameters to the fit.
5. Add the  $2\theta$  zero correction to the fit.
6. Use constraints to group  $U_{iso}$  parameters for like atoms; constrain the  $z$  parameters for Fe2a and Fe2b so that the atoms move in opposite directions and for O 1a and O 1b so the atoms move in the same direction. Finally, using EXPEDT, fix the nonzero parameters for the remaining four O atoms [L A F I 9 X I 10 Y I 11 Y I 12 X].
7. In EXPGUI, fit structural parameters (coordinates,  $U_{iso}$  values, and, where appropriate, fractional occupancies) as well as the background, scale, lattice, and  $2\theta$  zero.

Then, magnetic scattering is enabled and the model is refined:

8. In EXPEDT, change the flag to include nuclear and magnetic scattering [P P M 1 B].
9. Enter the color flags for the two red magnetic symmetry operations [L A M S C 2 C 3], and set moments for the atoms [L A M M 3 3.5 M 4 -3.5 M 5 -3.5 M 6 3.5].

10. Check/input the magnetic form factor [L F M F E +3 C .3972 13.244 .6295 4.903 -.0313 .35 0 0 .0044 N U].
11. Refine using EXPGUI, now including magnetic scattering (but no extra refined parameters).
12. Refine adding GU, GV, and GW (U,V, and W) to the model.
13. In EXPEDT, constrain the magnetic moments of the four Fe atoms to be the same (allowing for the differences in direction), and then set the refinement flag for the magnetic Fe atoms [L A P 2 V 1:4 M]; refine with these additional parameters.

## V. VERIFYING AND VISUALIZING MAGNETIC STRUCTURES

When using any crystallographic software, an important step is the verification that the supplied input generates the desired structure. For nuclear structures, this is usually done by checking interatomic distances and angles and by visualizing the structure. A similar check should be performed with magnetic structures and symmetry. The following examples show mechanisms for doing this. A set of accompanying web pages go through the same steps, but provide considerably more detail (see <http://www.ncnr.nist.gov/xtal/software/magtu>).

### A. Listing generated spins

To verify the spin directions for all magnetic atoms generated from symmetry, a routine has been added to the GSAS GEOMETRY program that lists the positions and magnetic vector components for the entire unit cell contents. This program can be accessed from the EXPGUI results menu.

Typical GEOMETRY input is:

1. Do not list the asymmetric unit contents for the initial phase [N].
2. Select the magnetic spin listing [M].
3. Choose a phase [P 2] (this step is omitted when only one phase is present).
4. Do not list the asymmetric unit contents for the selected phase [N].
5. Exit the program [X].

### B. Visualizing spins with VRSTPLOT

To visualize the magnetic spin directions, the program VRSTPLOT in GSAS can be used to generate a VRML graphics file that can then be visualized in a special viewer. The version of VRML (1.0) used by VRSTPLOT has been superseded, first by VRML97 (also called VRML 2.0) and now by a new standard, X3D. A viewer for VRML is not distributed with GSAS—in fact, one of the authors (B. H. T.) has been unable to locate a compatible viewer for OS X on the Macintosh, but has had success with an inexpensive program that converts VRML 1.0 files to VRML97 (<http://www.parallelgraphics.com/products/converter97>). For Windows, two freely distributed viewers that have been known to work with the VRML files produced by VRSTPLOT are: VRweb (<http://www.ccp14.ac.uk/ccp/ccp14/ftp-mirror/gsas/>

<http://www.ccp14.ac.uk/ccp/ccp14/ftp-mirror/gsas/public/gsas/windows/vrweb.exe>, <http://www2.iicm.edu/vrweb>) and CosmoPlayer (<http://ovrt.nist.gov/cosmo>). More information on VRML viewers is available from the Web3D consortium (<http://www.web3d.org>); their web page of VRML viewers ([http://www.web3d.org/x3d/vrml/tools/viewers\\_and\\_browsers](http://www.web3d.org/x3d/vrml/tools/viewers_and_browsers)) is extensive. Once a VRML browser has been installed, creation of VRML files with VRSTPLOT is relatively simple, as outlined below.

Input for a typical VRSTPLOT run is:

1. Select a phase [2] (this step is omitted when only one phase is present).
2. Enter the submenu to designate the atoms that will be plotted [A].
3. Add atoms to the view by designating a range of unit cell coordinates [U].
4. Use atoms 1 through 4 that fall between fractional coordinates 0 and 1 on all three axes [1:4 0 1 0 1 0 1].
5. Exit from add atoms menu [X].
6. Draw the unit cell boundary in the plot [U].

### C. Visualizing spins with DRAWxtl

To visualize the magnetic spin directions, input can also be created for the DRAWxtl program (Finger *et al.*, 2005) DRAWxtl is freely available for all platforms where GSAS runs and can directly display graphics on a computer screen. The program can also create either VRML 1.0 or VRML97 files, as well as input for POVRAY, which can be used to create very high quality, ray-traced, graphics output.

Input can be generated for the DRAWxtl program using a menu available in the EXPGUI Import/Export menu under the Coordinate Export submenu. From this menu, several options for display of atoms and magnetic spins can be selected, as shown on the accompanying web pages. Many additional display options are available within the DRAWxtl GUI, and even more capabilities are available by editing the DRAWxtl input file directly.

## VI. CONCLUSIONS

This article has shown three different approaches to modeling magnetic scattering using GSAS. The best approach to use will likely depend on the complexity of the material being studied. Researchers doing extensive work with magnetic scattering will likely want to master the Full-Prof program, but in many cases, such as the one shown here, GSAS offers an easy way to get started with magnetic refinements.

## ACKNOWLEDGMENTS

One of the authors (B. H. T.) wishes to thank Dr. Robert B. Von Dreele and Dr. Allen C. Larson for their efforts in creating the GSAS suite of programs as well as for many useful discussions over many years of fruitful interactions. Discussions with Professor Andrew S. Wills were also quite instructive, as were comments from many people who read early drafts of this work. Use of the Advanced Photon Source was supported by the U.S. Department of Energy, Office of Science, Office of Basic Energy Sciences, under Contract

No. W-31-109-ENG-38. Certain commercial products are identified to document experimental procedures. Such identification is not intended to imply recommendation or endorsement by the National Institute of Standards and Technology, nor is it intended to imply that these products are necessarily the best available for this purpose.

- Billiet, Y., Aroyo, M. I., and Wondratschek, H. (2004). "Tables of maximal subgroups of the space groups," *International Tables for Crystallography, Volume A1: Symmetry Relations Between Space Groups*, edited by H. Wondratschek and U. Müller (Kluwer, Dordrecht), pp. 153–154.
- Brown, P. J. (1995). "Magnetic form factors," *International Tables for Crystallography, Volume C: Mathematical, Physical and Chemical Tables*, edited by A. J. C. Wilson (Kluwer, Dordrecht), pp. 391–398.
- Cox, D. (1972). "Neutron-diffraction determination of magnetic structures," *IEEE Trans. Magn.* **8**, 161.
- Donnay, G., Corliss, L. M., Donnay, J. D. H., Elliott, N., and Hastings, J. M. (1958). "Symmetry of magnetic structures: Magnetic structure of chalcopyrite," *Phys. Rev.* **112**, 1917.
- Finger, L. W., Kroeker, M., and Toby, B. H. (2005). Home Page for DRAWxtl (<http://www.lwfinger.net/drawxtl>).
- Fultz, B. and Billinge, S. J. L. (2004). DANSE project diffraction software need survey (<http://danse.cacr.caltech.edu/polls/results.php?sid=22>).
- Heesch, H. (1930). "Über der vierdimensionalen Gruppen des Dreidimensionalen Raumes," *Z. Kristallogr.* **73**, 325–345.
- Huang, Q., Karen, P., Karen, V. L., Kjekshus, A., Lynn, J. W., Mighell, A. D., Rosov, N., and Santoro, A. (1992). "Neutron-powder-diffraction study of the nuclear and magnetic structures of  $\text{YBa}_2\text{Fe}_3\text{O}_8$  at room temperature," *Phys. Rev. B* **45**, 9611–9619.
- Iziumov, I. A. and Syromiatnikov, V. N. (1990). *Phase transitions and crystal symmetry* (Kluwer, Dordrecht, Netherlands).
- Karen, P., Kjekshus, A., Huang, Q., Karen, V. L., Lynn, J. W., Rosov, N., Sora, I. N., and Santoro, A. (2003). "Neutron Powder Diffraction Study of Nuclear and Magnetic Structures of Oxidized and Reduced  $\text{YBa}_2\text{Fe}_3\text{O}_{8+\delta}$ ," *J. Solid State Chem.* **174**, 87–95.
- Kovalev, O. V. (1993). *Representations of the Crystallographic Space Groups: Irreducible Representations, Induced Representations and Corepresentations* (Gordon and Breach, Amsterdam).
- Larson, A. C. and Von Dreele, R. B. (2000). Report No. LAUR 86-748. Los Alamos National Laboratory.
- Prince, E. (1994). *Mathematical Techniques in Crystallography and Materials Science* (Springer, New York).
- Rietveld, H. M. (1969). "A profile refinement method for nuclear and magnetic structures," *J. Appl. Crystallogr.* **2**, 65–71.
- Rodríguez-Carvajal, J. (1993). "Recent advances in magnetic structure determination by neutron powder diffraction," *Physica B* **192**, 55–69.
- Rodríguez-Carvajal, J. (2004). *BasiReps*, version 3.70. (<ftp://ftp.cea.fr/pub/lb/divers/BasIreps>).
- Shirane, G. (1959). "A note on the magnetic intensities of powder neutron diffraction," *Acta Crystallogr.* **12**, 282–285.
- Shubnikov, A. V. and Belov, N. V. (1964). *Colored Symmetry* (Oxford, Pergamon, New York).
- Sikora, W., Bialas, F., and Pytlik, L. (2004). "MODY: A program for calculation of symmetry-adapted functions for ordered structures in crystals," *J. Appl. Crystallogr.* **37**, 1015–1019.
- Stokes, H. T. and Hatch, D. M. (2002). *ISOTROPY*. (<http://stokes.byu.edu/isotropy.html>).
- Toby, B. H. (2001). "EXPGUI, a Graphical User Interface for GSAS," *J. Appl. Crystallogr.* **34**, 210.
- Vainshtein, B. K. (1996). *Fundamentals of Crystals, Symmetry, and Methods of Structural Crystallography* (Springer, New York).
- Wills, A. S. (2000). "A new protocol for the determination of magnetic structures using simulated annealing and representational analysis (SARAH)," *Physica B* **276**, 680–681.
- Wills, A. S. (2002). "Symmetry and magnetic structure determination: developments in refinement techniques and examples," *Appl. Phys. A: Mater. Sci. Process.* **74**, S856–S858.